



# Quantitative analysis of the major linkage region tetrasaccharides in heparin



Yin Chen<sup>a,b,\*</sup>, Kalib St.Ange<sup>b</sup>, Lei Lin<sup>b</sup>, Xinyue Liu<sup>b,c</sup>, Xing Zhang<sup>b</sup>, Robert J. Linhardt<sup>b,\*</sup>

<sup>a</sup> College of Food and Pharmacy, Zhejiang Ocean University, Zhoushan, Zhejiang 316000, China

<sup>b</sup> Departments of Chemistry and Chemical Biology, Biology, Chemical and Biological Engineering, and Biomedical Engineering, Center for Biotechnology and Interdisciplinary Studies, Rensselaer Polytechnic Institute, Troy, NY 12180, USA

<sup>c</sup> National Glycoengineering Research Center, Shandong Provincial Key Laboratory of Carbohydrate Chemistry and Glycobiology, and State Key Laboratory of Microbial Technology, Shandong University, Jinan, Shandong 250100, China

## ARTICLE INFO

### Article history:

Received 13 August 2016

Received in revised form

26 September 2016

Accepted 26 September 2016

Available online 29 September 2016

### Keywords:

Heparin linkage region

Peptidoglycosaminoglycan

Oxidized serine

Structural characterization

Mass spectrometry

Nuclear magnetic resonance spectroscopy

## ABSTRACT

Heparin is a polysaccharide based anticoagulant drug composed of a complex mixture of glycosaminoglycan chains and peptidoglycosaminoglycan chains. In an effort to better characterize this important polysaccharide based drug, we examined the peptide components of the minor peptidoglycosaminoglycan chains comprising heparin. Three different the glycan-peptide linkage regions tetrasaccharide fragments were isolated from pharmaceutical heparin using heparin lyase II and characterized the structure of these tetrasaccharides using nuclear magnetic resonance spectroscopy and mass spectrometry. A sensitive and quantitative assay was developed for these linkage regions using multiple reaction-monitoring tandem mass spectrometry. These three different linkage regions were found in heparins coming from porcine intestine and bovine lung. Two of these were also present in the low molecular weight heparin, enoxaparin.

© 2016 Elsevier Ltd. All rights reserved.

## 1. Introduction

Heparin is biosynthesized as a proteoglycan (PG) in the endoplasmic reticulum and Golgi compartments of granulated mast cells (Esko & Selleck, 2002; Horner, 1986; Rönnberg & Pejler, 2012). As many as 10 polysaccharide or glycosaminoglycan (GAG) chains of approximately 100 kDa are attached to the serine residues of a core protein serglycin, making the heparin PG a macromolecule with a molecular weight of approximately a million (Horner, 1986). These GAG chains are comprised of repeating 1→4-linked sulfated disaccharide units of uronic acid (either  $\alpha$ -L-iduronic acid (IdoA) or  $\beta$ -D-glucuronic acid (GlcA)) and  $\alpha$ -D-glucosamine (GlcN) residues. Mast cells are involved in the allergic response and, when an allergen bridges two immunoglobulin-type E molecules on the surface of the mast cell, the contents of the granules, including vasoactive amines (i.e., histamine) and heparin are released (Rönnberg & Pejler, 2012). The heparin released from mast cells is not the PG form but is instead a mixture of shorter GAG chains of approximately 16 kDa and peptidoglycosaminoglycan (pG) chains that

contain remnants of the core protein as a result of proteolytic processing and the action of heparanase, an endoglucuronosyl hydrolase (Rönnberg & Pejler, 2012; Vlodayky, Blich, Li, Sanderson, & Ilan, 2013).

While the biological functions of heparin are unclear, they are believed to be associated with response to infectious disease, particularly parasitic infections (Kamhi et al., 2013). Heparin, discovered exactly 100 years ago in an extract from canine liver (Linhardt, 1991, 2003), is widely used pharmacologically as an anti-coagulant drug and is critical to the practice of modern medicine (Onishi, St.Ange, Dordick, & Linhardt, 2016). Today heparin is prepared on the metric ton scale from porcine intestine, bovine intestine, bovine lung, and ovine intestine, all tissues that are rich in mast cells (Bhaskar et al., 2012; Fu et al., 2013). The process of purification of the raw heparin obtained from animal tissue to a refined pharmaceutical heparin generally involves some harsh chemical steps including base treatment (Bhaskar et al., 2012; Liu & Perlin 1992) and bleaching, through treatment with peracetic acid or hypochlorite, which can introduce structural artifacts (Beccatiet al., 2010; Li et al., 2014). Moreover, today much of the heparin produced in such processes is converted through controlled chemical or enzymatic depolymerization to low molecular weight (LMW) heparins, of approximately 4 kDa to 6 kDa, with improved bioavail-

\* Corresponding authors.

E-mail addresses: [cheny40@rpi.edu](mailto:cheny40@rpi.edu) (Y. Chen), [linhar@rpi.edu](mailto:linhar@rpi.edu) (R.J. Linhardt).

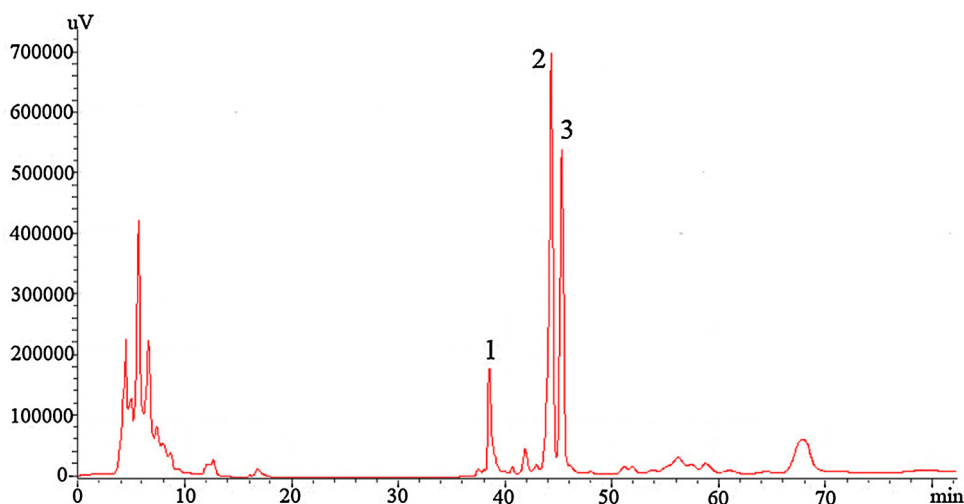


Fig. 1. HPLC of the purification of the tetrasaccharides in linkage region.

ability and pharmacodynamics properties (Fareed et al., 2004; Linhardt, 2003; Linhardt & Gunay, 1999). Despite the widespread medical use of heparin and LMW heparins and the biological significance of heparin, there is much that we still do not know about its structure (Linhardt, 2003; Li et al., 2014, 2015).

The objective of the current study is to identify a portion of the complex mixtures comprising heparin and LMW heparin products that can serve as a reporter of the severity of the oxidative and bleaching steps used in their manufacture (Bhaskar et al., 2012). The exact process conditions used to manufacture a heparin or LMWH are only well known to their manufacturer and these are trade secrets. When a new generic product (either heparin or LMWH) is introduced into the marketplace the only way to compare it to previously approved generic or innovator products is through its structural analysis. This is important as the structural properties of heparin or LMWH affects its bioactivity or bioavailability.

The current study examines the residual pG heparin chains that make it through the processing steps used to prepare pharmaceutical heparins and LMW heparins. Based on our understanding of the biosynthetic pathway of heparin PG, these pG chains are expected to contain a linkage region where the polysaccharide or GAG chain is connected to the serglycin core protein of the  $\rightarrow \beta$ -D-GlcA (1  $\rightarrow$  3)  $\beta$ -D-galactose (Gal) (1  $\rightarrow$  3)  $\beta$ -D-Gal (1  $\rightarrow$  4)  $\beta$ -D-xylose (Xyl) (1  $\rightarrow$  O-serine (Ser) (Esko & Selleck, 2002). The amount and the structural modifications to the linkage region tetrasaccharides should specifically reflect the process conditions in the preparation of pharmaceutical heparin and LMW heparin and might be useful for process control and regulatory concerns (Szajek et al., 2016). Fragments of the pG components of commercial heparin products were prepared enzymatically and identified by mass spectrometry (MS) and nuclear magnetic resonance (NMR) spectroscopy and a high performance liquid chromatography (HPLC)-MS method was developed for the quantitative analysis of the major linkage region tetrasaccharides present in pharmaceutical heparin products.

## 2. Materials and methods

### 2.1. Materials

*Escherichia coli* expression and purification of the recombinant *Flavobacterium heparinum* heparin lyase II (no EC assigned) was performed in our laboratory as described previously (Su et al., 1996). Pharmaceutical heparin samples were obtained from a variety of commercial suppliers, and LWM heparin samples were obtained

from a variety of commercial suppliers. All other chemicals were of HPLC grade.

### 2.2. Enzymatic digestion

A 500 mg (20 mg/mL) porcine intestinal heparin sodium (200 U/mg, Celsus) was dissolved in 50 mM sodium phosphate buffer (pH 7.4) and exhaustively digested by heparin lyase II (35 IU, activity acting on heparin) in 37 °C for 24 h. The enzymes were removed by centrifugation (8000g) through a 3 kDa MWCO spin column. Buffer salts and disaccharides present within the product mixture were removed by a P2 size exclusion column (Bio-Rad) (100  $\times$  2.0 cm) and lyophilized. The sample, containing tetrasaccharides, was detected using NanoDrop ND-1000 ultraviolet (UV)-visible (Vis) spectrophotometer (Thermo Scientific) at 232 nm.

### 2.3. Purification of the linkage region tetrasaccharides

The sample (5 mg in 100  $\mu$ L) obtained from enzymatic digestion and size exclusion chromatography was injected onto a Spherisorb-strong anion exchange (SAX) chromatography column (250  $\times$  20 mm), Waters, USA). Mobile phase A was water adjusted to pH 3.5 and mobile phase B was 2 M aqueous sodium chloride adjusted to pH 3.5. A linear gradient of mobile phase B ( $t_{0-20}$  min 0%;  $t_{20-120}$  min 15%–17%;  $t_{120-140}$  min 60%) was applied with a flow rate of 4 mL/min. Continuous UV detection was performed at 232 nm. All the peaks were collected and concentrated. The collected samples were desalted by P2 size exclusion column (100  $\times$  2.0 cm) and lyophilized.

### 2.4. NMR of the tetrasaccharides

Lyophilized samples were dissolved in 400  $\mu$ L of D<sub>2</sub>O and lyophilized, then re-dissolved in 400  $\mu$ L of D<sub>2</sub>O (99.96 atom%) and transferred to a 5-mm NMR tube. <sup>1</sup>H NMR (8 scans) and heteronuclear multiple quantum correlation (HMQC) NMR was performed on a Bruker 800-MHz NMR spectrometer, and acquisition of the spectra was carried out using Topspin 2.1.6 software. All spectra were acquired at a temperature of 298 K.

### 2.5. MS analysis of the tetrasaccharides

Electrospray ionization (ESI)-LTQ-Orbitrap-Fourier transform (FT) mass spectrometer (Thermo Fisher Scientific, San-Jose, CA) was

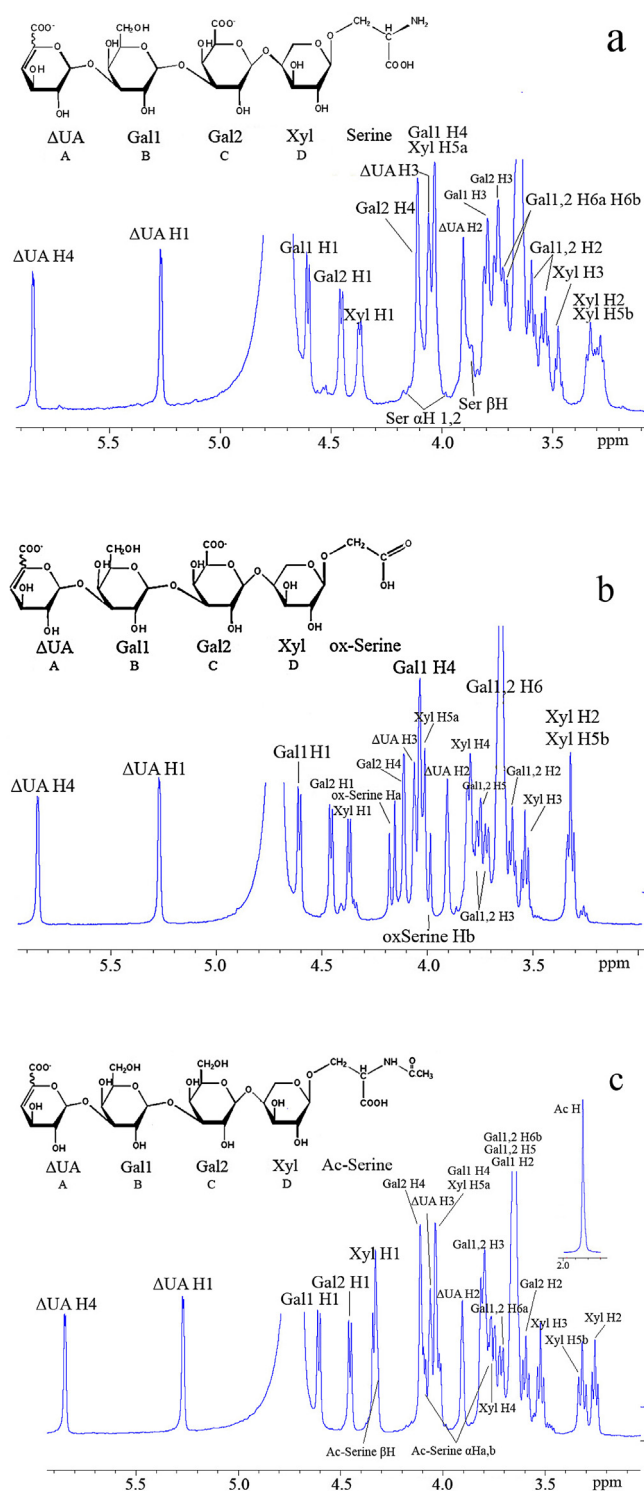


**Fig. 2.** 1D  $^1\text{H}$  NMR spectra of linkage region tetrasaccharides and their structures. a. 1D  $^1\text{H}$  NMR and structure of peak 1. b. 1D  $^1\text{H}$  NMR and structure of peak 2. c. 1D  $^1\text{H}$  NMR and structure of peak 3.

used to analyze the structure of the linkage region tetrasaccharides. Mobile phase A was 5 mM ammonium acetate prepared with HPLC grade water. Mobile B was 5 mM ammonium acetate prepared in 98% HPLC grade acetonitrile with 2% of HPLC grade water. The gradient was used 50% A at a flow rate of 250  $\mu\text{L}/\text{min}$ . The parameters, used to prevent in-source fragmentation, included a spray voltage of 4.2 kV, a capillary voltage of  $-40\text{ V}$ , a tube lens voltage of  $-50\text{ V}$ , a capillary temperature of  $275^\circ\text{C}$ , a sheath flow rate of 30 L/min,

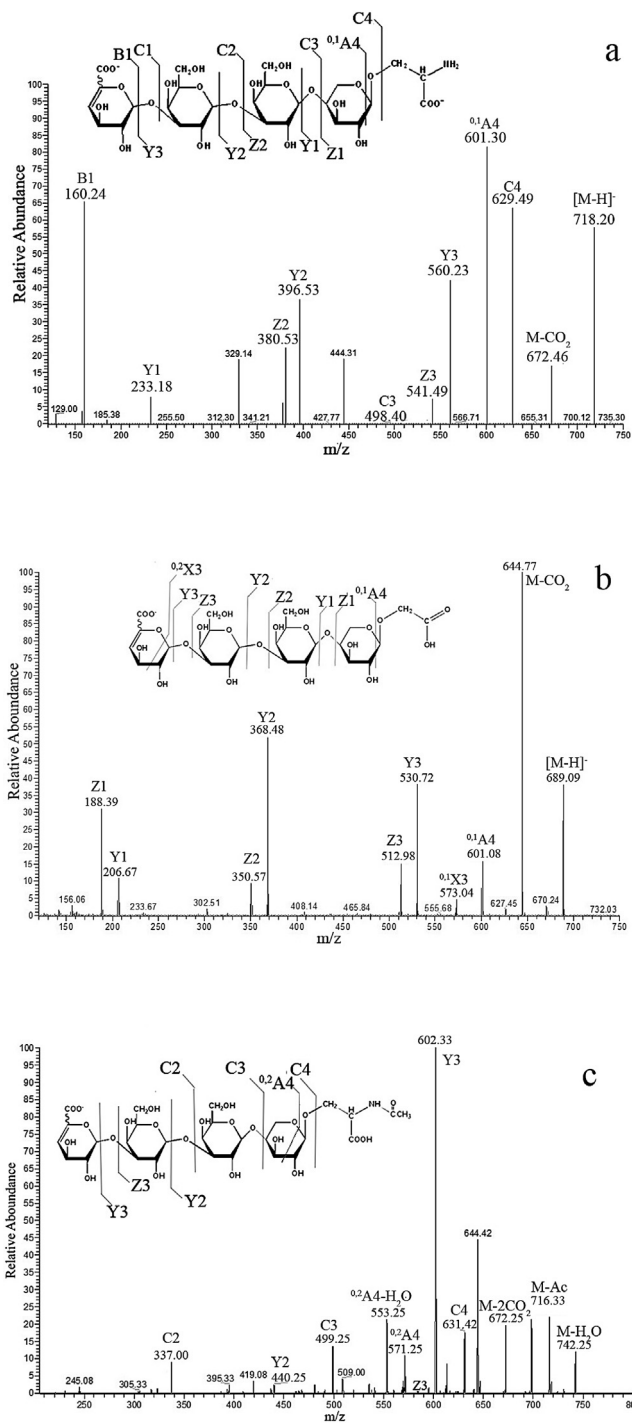


**Fig. 3.** Mass spectral analysis of linkage region tetrasaccharides. a. MS/MS of peak 1. b. MS/MS of peak 2. c. MS/MS of peak 3.

and an auxiliary gas flow rate of 6 L/min. External calibration of mass spectra routinely produced a mass accuracy of better than 3 ppm. All FT mass spectra were acquired at a resolution 60 000 with 200–2000 Da mass range.

## 2.6. Liquid chromatography tandem mass spectrometry

HPLC was performed on an Agilent 1200 LC system at  $45^\circ\text{C}$  using an Agilent Poroshell 120 ECC18 ( $2.7\ \mu\text{m}$ ,  $3.0 \times 50\text{ mm}$ ) column. Mobile phase A was 50 mM ammonium acetate aqueous solution, and the mobile phase B was methanol. The mobile phase

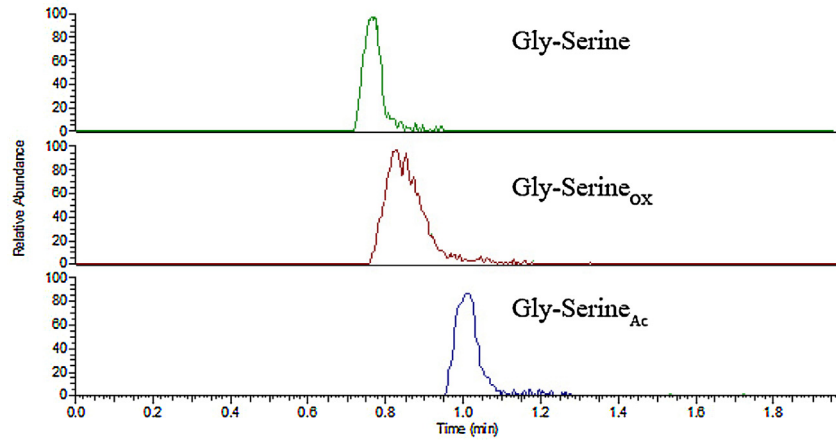


Fig. 4. Extracted ion chromatograms (EIC) of the three linkage region tetrasaccharides.

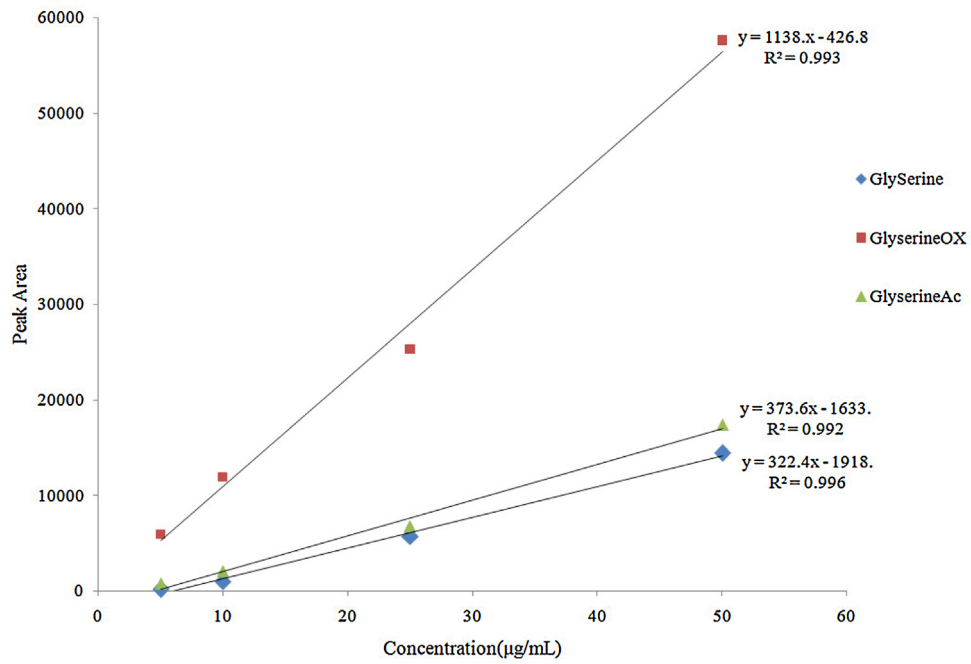


Fig. 5. MRM standard curves prepared using three linkage region tetrasaccharides.

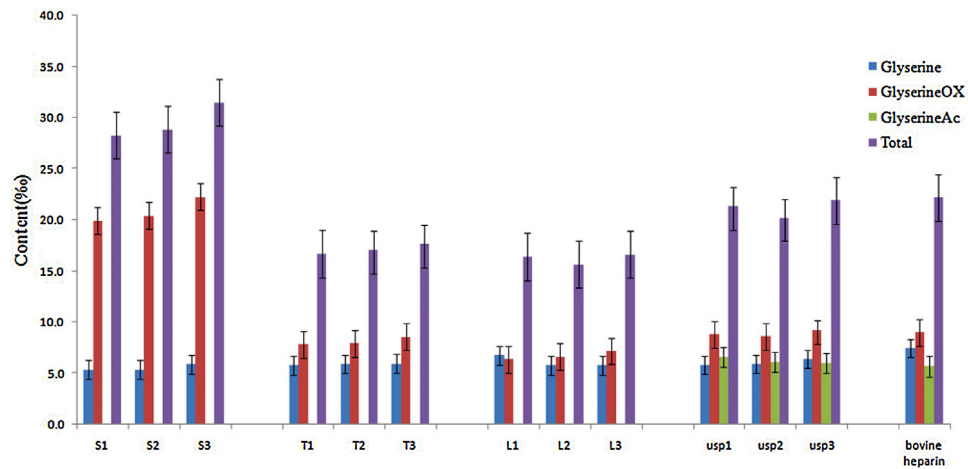


Fig. 6. Composition and comparison of three linkage region tetrasaccharides from different heparin and LMWHs (S1–S3, enoxaparin from Sandoz, T1–T3, enoxaparin from Teva; L1–L3 Lovenox®; USP 1–3, USP heparin from porcine intestine; bovine lung heparin was from bovine lung). The standard deviation of three injections of each sample is shown on each bar.

**Table 1**  
MRM conditions for Glycerin, Glycerin<sub>ox</sub> and Glycerin<sub>Ac</sub>.

sample	Precursor ion ( <i>m/z</i> )	Production ion	collisional energy (V)	tube len (V)	retention time (min)
Glycerin	718	673	38	−90	0.76
Glycerin <sub>ox</sub>	689	645	35	−100	0.85
Glycerin <sub>Ac</sub>	760	602	30	−100	1.0

passed through the column at a flow rate of 300  $\mu\text{L}/\text{min}$ . The content of MPB was 5%. A triple quadrupole mass spectrometry system equipped with an ESI source (Thermo Fisher Scientific, San Jose, CA) was used a detector. The online MS analysis was at the multiple reaction-monitoring (MRM) mode. The conditions and collision energies for the all of the disaccharides MRM transitions are listed in Table 1.

### 2.7. Heparin samples preparation

Three lots of porcine intestinal heparin active pharmaceutical ingredients (API) from Celsus and three lots of desalted and dialyzed LMWH drug products (100  $\mu\text{g}$ ) from three different manufacturers (Enoxaparin from Sandoz, Enoxaparin from Teva, Lovenox<sup>®</sup>) were dissolved in 100  $\mu\text{L}$  of distilled water and completely digested by heparin lyase II (20 mU) at 37  $^{\circ}\text{C}$  for 12 h. After reaction complete (no further change in UV absorbance at 232 nm), the enzyme was removed by centrifugation through a 3 kDa molecule weight cut-off (MWCO) spin column down at 12,000 rpm. The filter unit was washed twice with 100  $\mu\text{L}$  of distilled water and the combined filtrate, containing the linkage region tetrasaccharides was lyophilized. Each sample was dissolved in 10  $\mu\text{L}$  of distilled water and directly analyzed by HPLC–MS.

## 3. Results and discussion

### 3.1. Purification

In the manufacturing process of heparin (Bhaskar et al., 2012), much of the protein is eliminated by proteolysis in an alkaline environment. In addition, protein, peptide and DNA in the raw heparin are also removed by treatment with strong alkaline and oxidizing agents in the bleaching process (Bhaskar et al., 2012). While heparin is quite stable to base and oxidants, during these steps, heparin can undergo minor structural modification, particularly in its linkage region (Li et al., 2014).

Certain linkages within heparin are known to be resistant to exhaustive digestion with heparin lyase II, these include the tetrasaccharide at the linkage region as well as tetrasaccharides derived from the antithrombin binding site in heparin that contain a 3-*O*-sulfo group on the GlcN residue at their non-reducing end (Xiao et al., 2011). From 500 mg of sodium heparin approximately 40 mg of desalted tetrasaccharides were obtained. The tetrasaccharides from the linkage region are well resolved from other resistant tetrasaccharides as they contain no sulfo groups and only a single carboxyl group. Thus, on HPLC–SAX they show short retention times eluting at low ionic strength (Fig. 1).

### 3.2. Structure of tetrasaccharide from NMR and MS

The first three peaks from HPLC after the injection front were collected (Fig. 1 peak 1, 2, and 3) and identified by MS and NMR as tetrasaccharides coming from the peptidoglycosaminoglycan linkage region. The MS of peak1 showed a molecular ion peak  $[\text{M}-\text{H}]^{-}$  of *m/z* 718.21 (Fig. S1). The one dimensional (1D)  $^1\text{H}$  NMR spectrum (Fig. 2a) and the two dimensional (2D) HSQC spectrum (Fig. S2) showed that the compound making up peak 1 had four anomeric protons, AH1 at the non-reducing end (NRE) (5.27 ppm),

BH1 (4.60 ppm), CH1 (4.45 ppm) and DH1 at the reducing end (RE) (4.37 ppm), and corresponded to a tetrasaccharide. A signal at 5.84 ppm in the same region corresponded to the AH4 of deoxy- $\beta$ -*L*-threo-hex-4-enopyranosiduronic acid ( $\Delta\text{UA}$ ). These data confirm the structure of peak 1 as the tetrasaccharide  $\Delta\text{UA-Gal-Gal-Xyl-O-Ser}$ , Glycerin, which is derived from the original, unmodified core protein linkage region of pG. This linkage region tetrasaccharide had been previously reported (Li et al., 2014; Liu et al., 1995). The compound making up peak 2, showed a molecular ion  $[\text{M}-\text{H}]^{-}$  of *m/z* 689.18 (Fig. S3). The 1D (Fig. 2b) and 2D NMR spectra (Fig. S4) showed that the compound corresponding to peak 2 had a structure similar to peak 1. The signals for the saccharide portion of the molecule were almost identical. Comparison of the signals corresponding to serine showed that this compound lacked the signal of CH. Based on NMR and MS analysis its structure was determined to be an oxidized serine residue with the same tetrasaccharide attached,  $\Delta\text{UA-Gal-Gal-Xyl-O-CH}_2\text{COOH}$ , Glycerin<sub>ox</sub>. The compound making up peak 2 showed a molecular ion peak  $[\text{M}-\text{H}]^{-}$  of *m/z* 760.20 (Fig. S5). The 1D (Fig. 2c) and 2D NMR (Figs. S6 and S7) spectra again suggested that the same tetrasaccharide was present as had been observed in the compounds from peaks 1 and 2. The anomeric protons of AH1 (5.27 ppm), BH1 (4.60 ppm), CH1 (4.45 ppm) and DH1 (4.34 ppm) were almost the same. MS analysis showed that the molecular weight of the compound corresponding to peak 3 was 42 amu greater than that of the compound corresponding to peak 1. A signal in the  $^1\text{H}$  NMR spectrum at 1.98 ppm in  $^1\text{H}$  NMR spectrum demonstrated the presence of methyl group and the HMQC spectrum showed that this methyl group was attached to a carbonyl group at 170 ppm in the  $^{13}\text{C}$  spectrum. Thus, the compound corresponding to peak 3 was identical to the compound corresponding to peak 1 except for the modification of the Ser residue through acetylation. The chemical shift of the proton of the  $\beta$  CH of serine increased from 3.85 ppm to 4.3 ppm without any changes in the other Ser signals showing that the amino group of Ser had been acetylated. The structure of the compound corresponding to peak 3 was determined to be  $\Delta\text{UA-Gal-Gal-Xyl-O-CH}_2\text{CH}(\text{NHCOCH}_3)\text{COOH}$ , Glycerin<sub>Ac</sub>. The assignments of all of the signals are shown in Table S1.

### 3.3. MS/MS of tetrasaccharides

MS/MS was used to confirm the structures of the three linkage region tetrasaccharides isolated from heparin. None of these tetrasaccharides had any sulfation. MS/MS provides a fast approach for the identification of even very small quantities of these three linkage region tetrasaccharides. These three tetrasaccharides showed very similar fragmentation patterns (Fig. 3a–c) with the major fragmentation peaks corresponding to through-glycosidic cleavages (B, C and Y, Z). Fragments corresponding to B and C cleavages were also similar. A C4 cleavage in Glycerin<sub>Ac</sub> at *m/z* 631.4 confirms that the acetylation modification did not occur in the sugar portion of the molecule as the same fragment C4 cleavage was observed in Glycerin. Thus, the MS/MS analysis is fully consistent with the structure determined for these three linkage region tetrasaccharides.



### 3.4. Quantitative analysis of the linkage region tetrasaccharides in heparin

Every pG chain within a heparin product on treatment with heparin lyase II affords a single linkage region tetrasaccharide. Thus the total amount of linkage region tetrasaccharides reflects the amount of pG chains as well as their stability to the processing conditions used in heparin isolation and purification. Furthermore, the distribution of the three different types of linkage regions also provides information on the process conditions used in heparin isolation and purification. Therefore, the quantification of these linkage region tetrasaccharides provide an important tool for monitoring the production of heparins and also potentially LMW heparins.

The quantification of the three linkage region tetrasaccharides was performed using a micro-carbazole assay with  $\Delta$ UA-GlcNAc (0.1 mg/mL) as a standard. Based on this assay, the three samples were prepared in various concentrations ranging from 1  $\mu$ g/mL to 200  $\mu$ g/mL as standards for HPLC–MS analysis. Because the tetrasaccharides from the linkage region had no sulfate groups, it was possible to use the same HPLC–MS method in MRM mode that had been previously successfully applied to heparin disaccharides analysis (Li et al., 2015) for the direct analysis of the samples.

The HPLC conditions, used for the three linkage region tetrasaccharides, did not afford their complete separation. Fortunately, MRM mode allowed the separation of these three samples based on their different molecular weights in a 2 min analysis (Fig. 4). A series of samples were prepared containing different concentrations of these tetrasaccharides and analyzed to evaluate the linearity of tetrasaccharide amount and the peak area. The tetrasaccharide peak areas showed good linearity over a range from 5  $\mu$ g/mL to 50  $\mu$ g/mL (Fig. 5). MRM provides a rapid analytical method to determine the amount of these linkage region tetrasaccharides in a heparin product. The different slopes of the three curves reflected the different ionization efficiencies for the tetrasaccharides in an ESI source. Glycerin<sub>OX</sub> showed the highest ionization efficiency possibly due to its higher negative charge.

### 3.5. HPLC–MS analysis of heparins and LMWHs

Three batches of Celsus heparin samples and LMW heparins were next completely digested with heparin lyases II in triplicate and the resulting linkage region tetrasaccharides were analyzed by HPLC–MS using MRM. The results of these analyses showed that the contents of these linkage region tetrasaccharides were different in different commercial heparins and LMW heparins (Fig. 6). The content of Glycerin was at the range of 0.5–0.8%. Glycerin<sub>OX</sub> was the major component in the three tetrasaccharides, which was at range of 0.6%–2.5%. Glycosein<sub>Ac</sub> was only present in porcine intestinal and bovine lung heparin samples but was not detected in any of the LMW heparins studied. We speculate that the acetyl group comes from the peracetic acid-bleaching step commonly used in producing pharmaceutical heparins (Mourier, Guichard, Herman, & Viskov, 2011). This acetyl residue or the modified serine might be selectively lost in the basic chemical  $\beta$ -elimination step used to produce LMW heparins (enoxaparins) from its parent heparin. Generic enoxaparin from Sandoz had the highest amount of Glycerin<sub>OX</sub> and highest total amount of linkage region tetrasaccharides, while Lovenox® (the innovator enoxaparin) had the lowest content of Glycerin<sub>OX</sub>. The composition of the tetrasaccharides was similar in the porcine intestinal and bovine lung heparins examined. The content of the tetrasaccharides from the linkage region did not vary much in different lots of LMW heparins examined coming from the same supplier.

## 4. Conclusions

While we have a general understanding of the process to prepare heparins and LMWHs, the specifics of individual manufacturing processes are trade secrets (Bhaskar et al., 2012; Linhardt & Gunay, 1999). Moreover, such process steps can also take place to the crude heparin, at either the slaughterhouse or consolidator levels, before it moves to a cGMP facility under regulatory oversight. This makes their detection only possible through forensic analysis. The analyses described in this manuscript provide some insights into the differences in such processes. The strength of the oxidation step can lead to the oxidation and the use of peracetic acid in the bleaching step can lead to acetylation of the serine residue in the pG chains of a heparin product. Thus, the modification of the serine residue can serve as an indication of these process steps. These pG chains are only present in very minor amounts within a heparin product, which is primarily composed of GAG chains. Thus, modern analytical methods together with the preparation of oligosaccharide standards offer an approach to better understand and ultimately control these process artifacts.

## Acknowledgements

The work was supported by Grants from the National Institutes of Health in the form of Grants HL125371, GM38060, GM090127, HL096972, and HL10172. This work was also supported in part by the China scholarship council.

## Appendix A. Supplementary data

Supplementary data associated with this article can be found, in the online version, at <http://dx.doi.org/10.1016/j.carbpol.2016.09.081>.

## References

- Beccati, D., Roy, S., Yu, F., Gunay, N. S., Linhardt, R. J., Capila, I., et al. (2010). Identification of a novel structure in heparin generated by potassium permanganate oxidation. *Carbohydrate Polymers*, 82, 699–705.
- Bhaskar, U., Sterner, E., Hickey, A. M., Onishi, A., Zhang, F., Dordick, J. S., et al. (2012). Engineering of routes to heparin and related polysaccharides. *Applied Microbiology and Biotechnology*, 93, 1–16.
- Esko, J. D., & Selleck, S. B. (2002). Order out of chaos: Assembly of ligand binding sites in heparan sulfate. *Annual Reviews in Biochemistry*, 71, 435–471.
- Fareed, J., Hoppensteadt, D., Schultz, C., Ma, Q., Kujawski, M. F., Neville, B., et al. (2004). Biochemical and pharmacologic heterogeneity in low molecular weight heparins. Impact on the therapeutic profile. *Current Pharmaceutical Design*, 10, 983–999.
- Fu, L., Li, G., Yang, B., Onishi, A., Li, L., Sun, P., et al. (2013). Structural characterization of pharmaceutical heparins prepared from different animal tissues. *Journal of Pharmaceutical Science*, 102, 1447–1457.
- Horner, A. A. (1986). Rat heparins A study of the relative sizes and antithrombin-binding characteristics of heparin proteoglycans, chains and depolymerization products from rat adipose tissue, heart, lungs, peritoneal cavity and skin. *Biochemical Journal*, 240(1), 171–179.
- Kamhi, E., Joo, E. J., Dordick, J. S., & Linhardt, R. J. (2013). Glycosaminoglycans in infectious disease. *Biological Reviews Cambridge Philosophical Society*, 88(4), 928–943.
- Li, G., Steppich, J., Wang, Z., Sun, Y., Xue, C., Linhardt, R. J., et al. (2014). Bottom-up LMWH analysis using LC-FTMS for extensive characterization. *Analytical Chemistry*, 86, 6626–6632.
- Li, G., Tian, F., Zhang, L., Xue, C., Li, L., & Linhardt, R. J. (2015). Glycosaminoglycanomics of cultured cells using a rapid and sensitive LC-MS/MS approach. *ACS Chemical Biology*, 10, 1303–1310.
- Linhardt, R. J., & Gunay, N. S. (1999). Production and chemical processing of low molecular weight heparins. *Seminars in Thrombosis and Hemostasis*, 25, 5–16.
- Linhardt, R. J. (1991). Heparin: An important drug enters its seventh decade. *Chemistry & Industry*, 2, 45–50.
- Linhardt, R. J. (2003). Heparin: Structure and activity. *Journal of Medicinal Chemistry*, 46, 2551–2554.
- Liu, Z., & Perlin, A. S. (1992). Adverse effects of alkali and acid on the anticoagulant potency of heparin: Evaluated with methyl 2-deoxy-2-sulfamino-alpha-D-glucopyranoside 3-sulfate as a model compound. *Carbohydrate Research*, 228(1), 29–36.

- Liu, J., Desai, U. R., Han, X.-J., Toida, T., & Linhardt, R. J. (1995). Strategy for the sequence analysis of heparin. *Glycobiology*, *5*, 765–774.
- Mourier, P. A., Guichard, O. Y., Herman, F., & Viskov, C. (2011). Heparin sodium compliance to the new proposed USP monograph: Elucidation of a minor structural modification responsible for a process dependent 2.10 ppm NMR signal. *Journal of Pharmaceutical and Biomedical Analysis*, *54*(2), 337–344.
- Onishi, A., St-Ange, K., Dordick, J. S., & Linhardt, R. J. (2016). Heparin and anticoagulation. *Frontiers in Bioscience*, *21*, 1372–1392.
- Rönnerberg, E., & Pejler, G. (2012). Serglycin: The master of the mast cell. *Methods in Molecular Biology* *836*, 201–217.
- Su, H., Blain, F., Musil, R. A., Zimmermann, J., Gu, K., & Bennett, D. C. (1996). Isolation and expression in *Escherichia coli* of hepB and hepC, genes coding for the glycosaminoglycan-degrading enzymes heparinase II and heparinase III, respectively, from *Flavobacterium heparinum*. *Applied and Environmental Microbiology*, *62*, 2723–2734.
- Szajek, A. Y., Chess, E., Johansen, K., Gratzl, G., Gray, E., Keire, D., et al. (2016). The US regulatory and pharmacopeia response to the global heparin contamination crisis. *Nature Biotechnology*, *34*, 625–630.
- Vlodavsky, I., Blich, M., Li, J. P., Sanderson, R. D., & Ilan, N. (2013). Involvement of heparanase in atherosclerosis and other vessel wall pathologies. *Matrix Biology*, *32*(5), 241–251.
- Xiao, Z., Tappen, B. R., Ly, M., Zhao, W., Canova, L. P., Guan, H., et al. (2011). Heparin mapping using heparin lyases and the generation of a novel low molecular weight heparin. *Journal of Medicinal Chemistry*, *54*, 603–610.